

Photoassociation adiabatic passage of ultracold Rb atoms to form ultracold Rb₂ molecules

Evgeny A. Shapiro,¹ Moshe Shapiro,^{1,2} Avi Pe'er,³ and Jun Ye³

¹*Department of Chemistry, University of British Columbia, Vancouver, Canada*

²*Department of Chemical Physics, Weizmann Institute of Science, Rehovot 76100, Israel*

³*JILA, National Institute of Standards and Technology*

and University of Colorado, Boulder, CO 80309-0440

Abstract

We theoretically explore photoassociation by Adiabatic Passage of two colliding cold ⁸⁵Rb atoms in an atomic trap to form an ultracold Rb₂ molecule in its ground ro-vibrational level. We consider the incoherent thermal nature of the scattering process in a trap and show that coherent manipulations of the atomic ensemble, such as adiabatic passage, are feasible if performed within the coherence time window dictated by the temperature, which is relatively long for cold atoms. By repeating the coherent process many times association of the entire thermal cloud can be achieved, yet care should be taken to remove the created molecules from the beam path between pulse sets. We show that a sequence of $\sim 2 \times 10^7$ pulses of moderate intensities, each lasting ~ 750 ns, can photoassociate a large fraction of the atomic ensemble at temperature of 100 μ K and density of 10^{11} atoms/cm³. Use of multiple pulse sequences makes it possible to populate the ground vibrational state.

I. INTRODUCTION.

The use of Adiabatic Passage (AP)[1, 2] to form ultracold molecules by photoassociating ultracold atoms[3, 4, 5, 6, 7] with Resonantly Enhanced Anti-Stokes Raman (REAR) pulses in counter-intuitive ordering is an attractive idea, mainly due to the promise of high yield. Central to the AP process is the formation of a “dark state” i.e., a light-dressed state that once formed, is impervious to further actions of the light fields. When the light fields are applied as pulses, AP results from the dark state changing its nature by following the makeup of the applied pulses from that of the input state (scattering state) to the desired final state (molecular bound state).

Unlike in conventional bound-bound AP (e.g. STIRAP) [1, 2], the input state in the photoassociation is not a pure state, but a thermal mixture of states. It can be represented as an incoherent mixture of different energy eigenstates, where the scenario of coherent manipulation proposed here works with similar efficiency for any initial energy within the thermal spread of the initial ensemble. Alternatively, the input state can be represented as a mixture Gaussian wave packets localized in phase space. The applied laser pulses in our scheme are not much longer than the coherence time of the thermal ensemble, which is equivalent to the average collision time of the coherent wave packets. Within the coherence time-window all initial states behave alike, and the coherent manipulation with these states succeeds.

Another difference between AP from the continuum and conventional three-level STIRAP due to the dynamical nature of the continuum is that while in STIRAP the input state can be completely transferred into the final state, in photoassociation this is not possible (only a small fraction of the atoms are colliding at a given time). Here however, the continuum serves as a coherent source / sink of population that is coupled by the light fields to the bound molecular states. By applying the coherent pulses over and over on the thermal ensemble of atoms, the overall photoassociation yield, which is an incoherent sum of yields from individual pulse sets, can approach unity on a reasonable time scale.

Although dark states connecting continuum and bound states have now been observed experimentally [8, 9], Photoassociation Adiabatic Passage (PAP) has not been realized so far. The main reason is that adiabaticity implies large “Rabi-frequencies”, which, due to the weakness of the bound continuum dipole-matrix-elements (controlled by the Franck-Condon

(FC) shape factors), imply the use of high intensity pulses. The production of high intensity in conjunction with relatively long pulse durations is not so easy to achieve in practice. In addition, the exact values of the pulse parameters are still under study [6].

This paper describes a set of realistic calculations of the $^{85}\text{Rb}+^{85}\text{Rb} \rightarrow ^{85}\text{Rb}_2$ photoassociation in an attempt to determine the pulse parameters needed to bring about PAP for this system. We use two pairs of pulses: The first of these pairs transfers the population from continuum to the fourth excited state of the $X^1\Sigma_g^+$ of Rb_2 (REAR). The second pair transfers the population to the ground vibrational state (conventional STIRAP). Special care is taken of averaging over the thermal ensemble of colliding atoms at $100 \mu\text{K}$ temperature, employing the laser pulses that photoassociate most initial states in the ensemble. We find that with sensible laser parameters photoassociation at a rate of $\sim 5 \times 10^{-8}$ per pulse is possible, which reflects the limit set by the sample density and temperature. Accordingly, photoassociation of a major fraction of the ensemble can be achieved by repeating the pulse sequence $\sim 2 \times 10^7$ times. In order to avoid excitation of the created molecules by subsequent pulses it is necessary to either remove them from the beam path or “hide” them via an irreversible process (e.g. spontaneous emission). We discuss the possibility of using a slowly moving optical lattice for that purpose. In the case of photoassociation of high phase-space density sample, it must be possible to photo-associate the whole sample with a single pulse sequence.

II. MOLECULAR DATA.

For notational simplicity we henceforth denote the $X^1\Sigma_g^+$ electronic state as “X”, and the spin-orbit-coupled $b^3\Pi_u$ and $A^1\Sigma_u$ potentials as “A/b”. We shall consider the photoassociation scenarios illustrated in Fig. 1, all starting with two ^{85}Rb atoms colliding on the Rb_2 X-potential. A pair of laser pulses transfers, using Resonantly Enhanced Anti-stokes Raman (REAR), a fraction of the incoming continuum population to an excited vibrational state of the Rb_2 X-state. The pair of pulses consists of a pump pulse, which couples the X-continuum to one of the A/b-bound states, and an Anti-Stokes dump pulse, which couples this A/b-bound state to an excited X-vibrational state. A second, much weaker, pair of pulses, which transfers (again by REAR, which in this case reduces to the bound-bound STIRAP[1, 2]) the population from the excited X-vibrational state to the ground vibrational

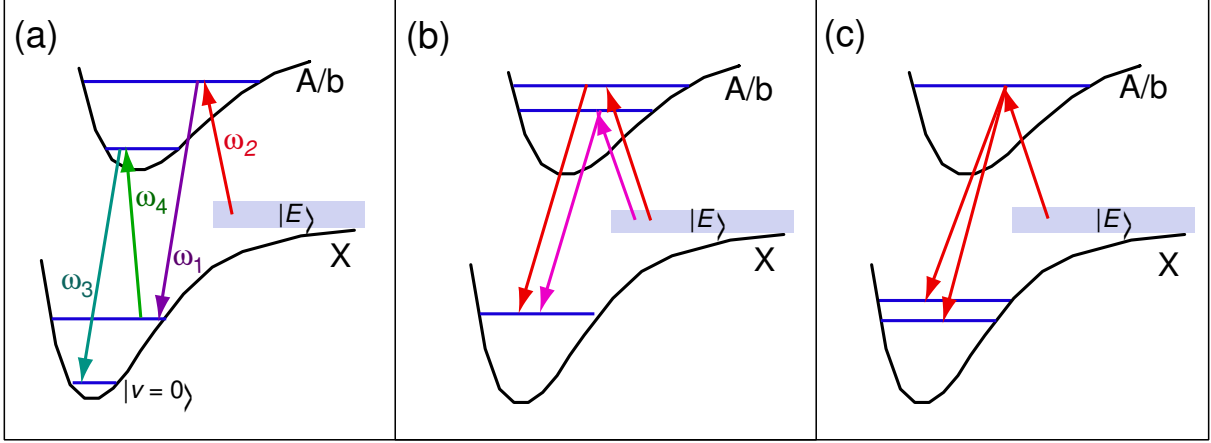


FIG. 1: (Color online). Three combinations of photoassociation adiabatic passage (PAP) pairs discussed in the text. (a) two-step REAR Photoassociation, (b) Interference between different REAR paths to control final state population, (c) Quantum state engineering via STIRAP / REAR.

state, then follows. Other scenarios which exploit the interferences between dark states in multi-pathway AP will also be discussed.

Fig. 2 shows the Born-Oppenheimer potentials used in the calculations. The X-potential at inter-atomic distances below 40 a.u. was taken from the Ref. [12], whereas at large distances the X-potential was modelled as a $-C_6/r^6$ dispersion term, with the value $C_6 = 4426$ a.u. taken from Ref. [13]. The short-term and the long-term potentials were smoothly interpolated near 40 a.u. The A/b potentials, and the spin-orbit coupling between them were adopted from Ref.[12].

The continuum-bound FC factors for the X-A/b transitions were calculated using the artificial channel method [18]. Their scaling was verified by comparison with that of the s-wave scattering wavefunction found by a simple outward propagation on the X-potential. Unlike bound-bound FCs, which are dimensionless overlap integrals, the free-bound FCs have dimensions of $(Energy)^{-1/2}$, due to the different normalization of free states.

The s-wave scattering of the two ^{85}Rb atoms on the X-potential at the energies of interest is influenced by a resonance, giving rise to a scattering length in excess of 2400 a.u. [14]. This resonance is due to the last (quasi-) bound state lying just a notch (above) below the continuum [15, 16]. We mention in passing that the collision of two ^{85}Rb atoms on the $1^3\Sigma_u$ potential is also influenced by a resonance, but to a lesser degree (scattering length of ~ 360

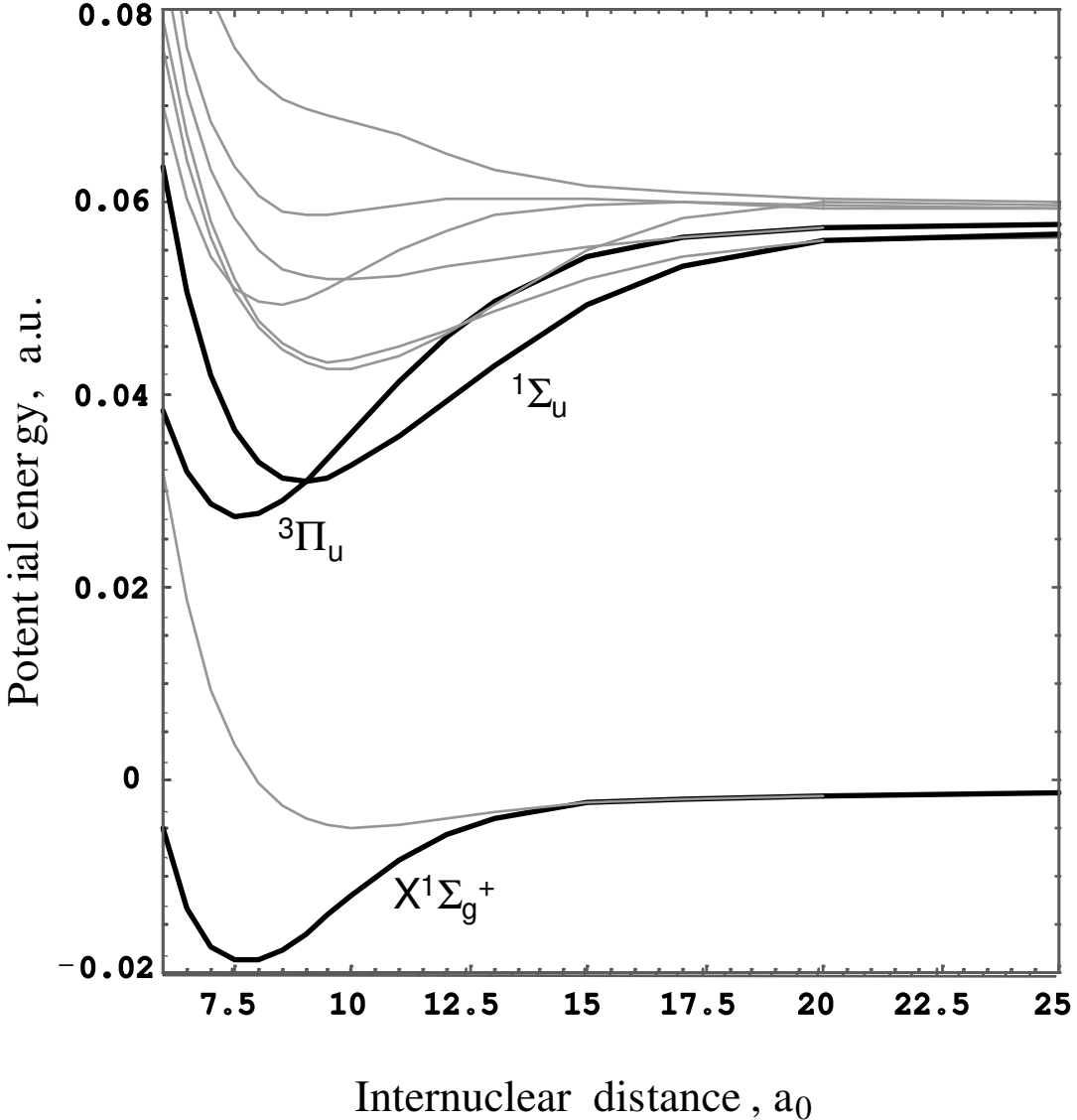


FIG. 2: Black lines: Rb_2 Born-Oppenheimer potentials involved in the photoassociation calculations. Gray lines: Rb_2 potentials not used in this paper. The data shown in the Figure are adopted from Ref.[17].

a.u.). In contrast, the collision of two ^{87}Rb atoms at the energy range below is not influenced by the resonance because it is sufficiently removed from it[14].

The existence of a scattering resonance affects our photoassociation scheme in two ways: First, the amplitude of the continuum wavefunction in the inner region is strongly enhanced relative to the non-resonant case. This enhances the X-A/b continuum-bound FC factors, with the required laser intensities being much lower than those needed in a non-resonant case.

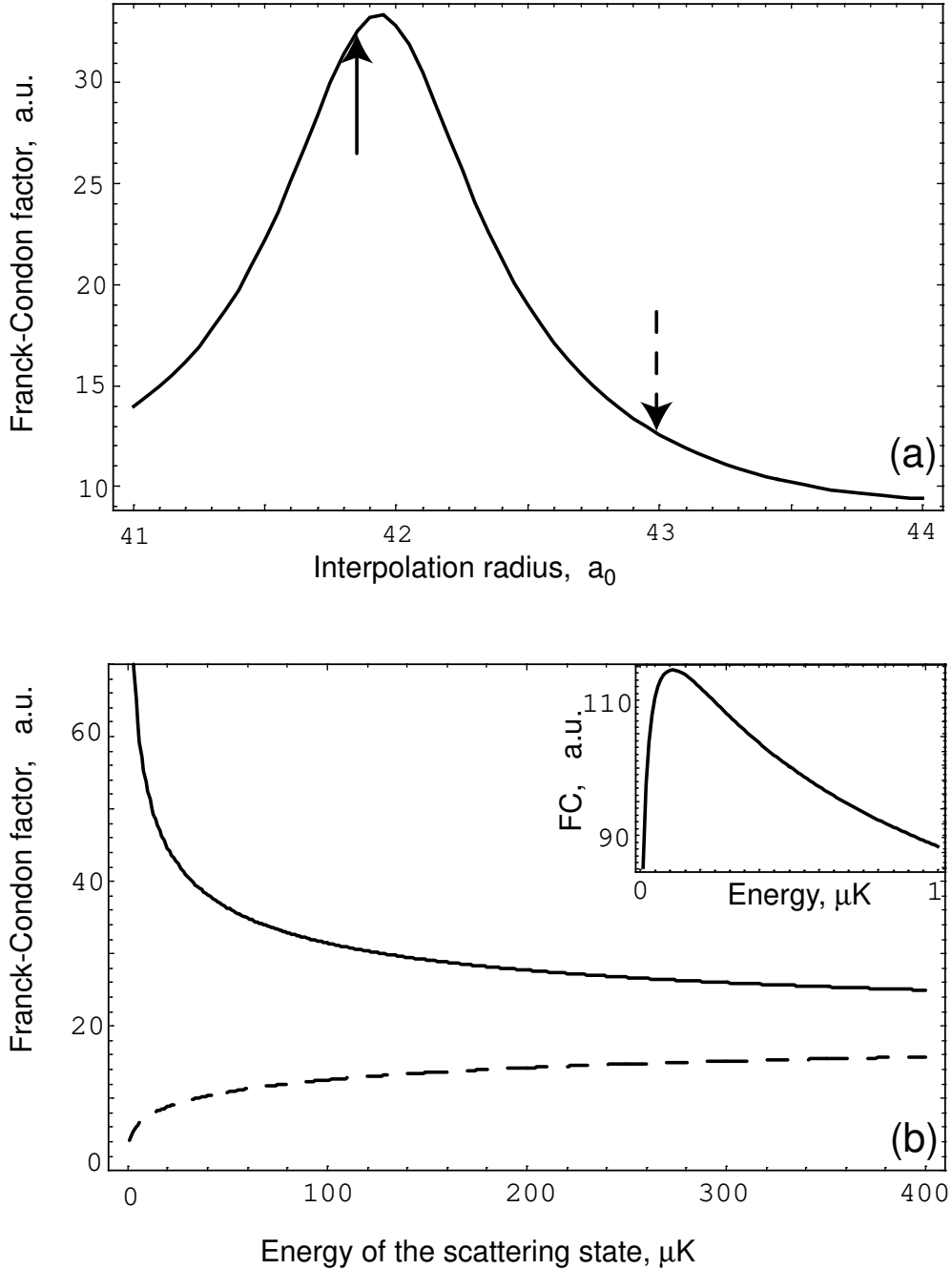


FIG. 3: (a) The Franck-Condon (FC) factors for the transition from a continuum state of $100 \mu\text{K}$ energy to the $\text{A}/\text{b}(133)$ level, for different X-potential long-range/short-range interpolation radii. The full arrow indicates the fitting parameter that correctly yields the measured scattering resonance and scattering length, which is used in further calculations. (b) The continuum-bound FC factors for the transition to the $\text{A}/\text{b}(v = 133, J = 1)$ level as a function of the scattering energy. The full (dashed) line corresponds to an interpolation radius marked by the full (dashed) arrow in (a). The inset shows the FC factor near the resonance at the $E = 0 - 1 \mu\text{K}$ continuum energy range.

Second, at near-resonance energies the $T(E) \sim E^{1/4}$ threshold law[16] does not hold. As a result the FC factors at very low energies are sufficiently high to ensure complete adiabatic transfer, with the PAP scheme expected to work for relatively low laser intensities.

The resonance features and the continuum-bound FC factors depend sensitively on the way the interpolation between the short range and long range forms of the X-potential is implemented. Fig. 3(a) shows the FC factor to the A/b($v = 133, J = 1$) ($E = 0.042848$ a.u.) bound state for initial scattering energy of $100 \mu\text{K}$ as a function of the X-potential interpolation radius. If the latter quantity is chosen around 42 a.u. (full arrow in Fig. 3(a)) the resulting scattering length is ~ 2500 a.u. When the interpolation radius is chosen as 43 a.u. (dashed arrow) the resonance moves slightly but sufficiently to change the scattering length to 100 a.u. The dependence of the FC factors on the collision energy is shown in Fig. 3(b). Away from the resonance the FC factors follow the Wigner law. The sensitivity of the FC factors to the interpolation radius diminishes at higher energies.

The dependence of the continuum-bound s-wave FC factors for scattering energy of $E = 100 \mu\text{K}$ on the bound A/b states energies is shown in Figure 4(a). The results can be explained using a semiclassical phase space analysis based on the Husimi or Wigner functions. This analysis shows that for the low-lying A/b states the classical closed phase space trajectories lie at low position and momentum values and do not intersect the X-state open collision trajectory, rendering the A/b-X FC factor exponentially small. In contrast, as the energy of the A/b states is increased, the X and A/b phase space trajectories start to overlap, thereby increasing the continuum-bound FC factors to several a.u.

The PAP scheme is expected to work conveniently for transitions to bound states lying in the vicinity of the A/b($v = 133, J = 1$) level ($E = 0.042848$ a.u.). This choice is based on the ability to generate large area (microsecond-long) pulses at wavelengths near $\sim 1064\text{nm}$, corresponding to the transition frequency to this state. The FC factor for the continuum-bound X-A/b($v = 133, J = 1$) transition, with initial scattering energy of $100 \mu\text{K}$ is equal to 31.5 a.u.

Another scenario [19, 20, 21, 22, 23] consists of using the set of the highly extended “sub-continuum” bound states existing just below the onset of the A/b continuum. The advantage here is that the continuum-bound FC factors associated with these states are higher by two or three orders in magnitude relative to the A/b($v = 133, J = 1$) region, allowing for the use of much weaker pump lasers. The disadvantage is that this scenario necessitates

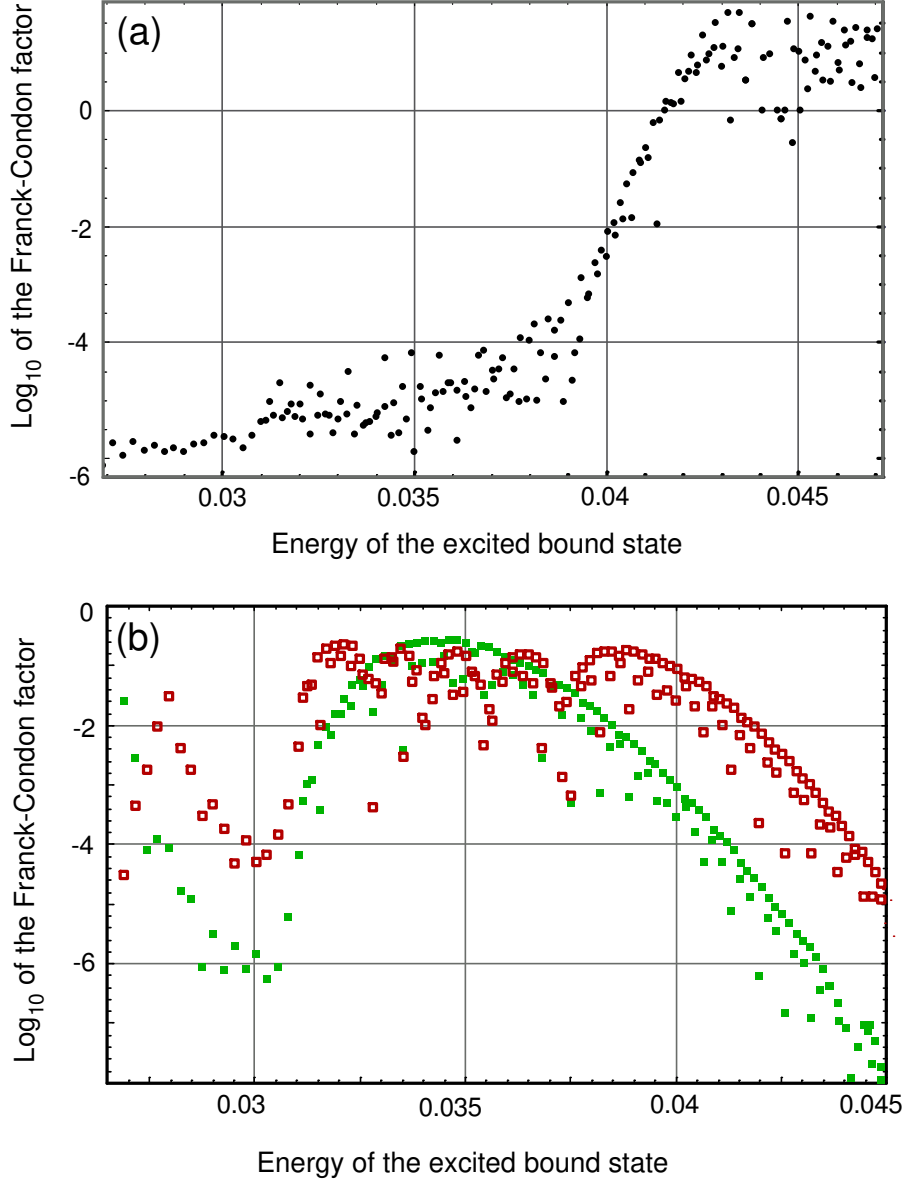


FIG. 4: (Color online). (a) FC factors for the X–A/b continuum-bound transitions. (b) FC factors for the A/b–X bound-bound transitions, for the $v = 0$ (green filled squares) and $v = 4$ (red open squares) X-vibrational states.

controlling the long-range behavior of the “sub-continuum” states, which in turn depends very strongly on the (poorly known) couplings between the many potentials which play a part in the dynamics. Moreover, the “sub-continuum” states greatly weaken the A/b–X FC factors associated with the dump pulse. Recent attempts to optimize photoassociation by controlling behavior of these states have not brought a clear answer on whether a significant optimization is possible[22, 23].

The eigenenergies of the coupled A/b bound states have been computed by the artificial channel method[18] and confirmed using the finite difference with Richardson extrapolation FDEXTR code[24]. The latter was used to compute the bound-bound X-A/b FC factors shown in Fig. 4(b).

In all the calculations reported below we estimate the X–A electronic-dipole moment to be $\mu = 3$ a.u. This value corresponds to the $5S_{1/2}(m = 1/2) - 5P_{3/2}(m = 3/2)$ transition in Rb atom in a circularly polarized field. It is consistent with all the other $5S - 5P$ matrix elements for Rb atom under the action of a polarized laser field. The exact values of the atomic reduced dipole matrix elements can be found in Ref. [25].

III. THEORY OF PHOTOASSOCIATION ADIABATIC PASSAGE

Following Ref. [3, 26], we express the total Hamiltonian of our system as

$$\hat{H} = \hat{H}_0 - 2\hat{\mu} \sum_{n=1}^2 \epsilon_n(t) \cos \omega_n t, \quad (1)$$

where \hat{H}_0 is the material Hamiltonian, $2\epsilon_n(t)$ are the (slowly varying) amplitudes of the coupling fields and $\hat{\mu}$ is the A/b–X electronic transition dipole moment. We expand the material wavefunction as

$$\psi = \sum_{i=1}^2 b_i e^{-iE_i t} |i\rangle + \int_{E_{th}}^{\infty} dE b_E e^{-iEt} |E\rangle, \quad (2)$$

where $|i\rangle$ and $|E\rangle$ are bound and continuum states of \hat{H}_0 , E_{th} is the threshold energy for the continuum states,

$$(E_i - \hat{H}_0) |i\rangle = (E - \hat{H}_0) |E\rangle = 0, \quad (3)$$

$i = 1$ ($i = 2$) denotes specific vibrational states in the X (A/b) electronic manifold, and $|E\rangle$ denotes a continuum state in the X electronic manifold. Atomic units ($\hbar = 1$) are used throughout.

We assume that the frequency ω_1 of the laser field is in near resonance with $\omega_{2,1} \equiv E_2 - E_1$ (see Fig. 1(a)) and that ω_2 is in near resonance with $\omega_{2,E} \equiv E_2 - E$, thus justifying the use of the Rotating Wave Approximation. The Schrödinger equation now assumes the simple

form [3, 26]

$$\dot{b}_1 = i \Omega_1^* b_2 e^{-i \Delta_1 t} \quad (4)$$

$$\dot{b}_2 = i \Omega_1 b_1 e^{i \Delta_1 t} - \Gamma_f b_2 + i \int_{E_{th}}^{\infty} dE b_E \Omega_E e^{i \Delta_2 t} \quad (5)$$

$$\dot{b}_E = i b_2 \Omega_E^* e^{-i \Delta_2 t} \quad (6)$$

where $\Delta_1 \equiv \omega_{2,1} - \omega_1$, $\Delta_2 \equiv \omega_{2,E} - \omega_2$ are the detunings and $\Omega_1 = \epsilon_1 \mu_{21}$, $\Omega_E = \epsilon_2 \mu_{2E}$ are the Rabi frequencies. The empirical term $\Gamma_f b_2$ describes the free decay of the $|2\rangle$ state. Since this free decay is predominantly to high energy continuum states (hot, untrapped atoms), it is assumed not to affect the continuum states $|E\rangle$.

Equations (4-6) can be simplified in the following standard way [3, 4]. Integrating Eq.(6) gives

$$b_E(t) = i \int_0^t dt' b_2(t') \Omega_E^*(t') e^{-i \Delta_2 t'} + b_E(t=0), \quad (7)$$

where the moment $t=0$ precedes the pulses. Upon substitution of this equation into Eq.(5) one obtains

$$\dot{b}_2 = i \Omega_1 b_1 e^{i \Delta_1 t} - \Gamma_f b_2 - \epsilon_2(t) \int_0^t dt' F_{corr}(t-t') \epsilon_2^*(t') b_2(t') + i \Omega_E F_0(t) \quad (8)$$

Here the spectral autocorrelation function

$$F_{corr}(t-t') = \int_{E_{th}}^{\infty} dE |\mu_{2E}|^2 e^{i \Delta_2 (t-t')} \quad (9)$$

is responsible for the field-induced decay from the state $|2\rangle$ and subsequent re-pumping from the continuum, and the source function

$$F_0(t) = \int_{E_{th}}^{\infty} dE b_E(0) e^{i \Delta_2 t} \quad (10)$$

gives the phase-space envelope [27] of the initial wave packet of continuum states with near-threshold energy.

Equation (8) can be further simplified by using the "flat", or "slowly varying continuum" approximation (SVCA), which assumes that Ω_E is constant within the range of continuum energies affected by the laser pulses and that E_{th} can be replaced with $-\infty$. In the calculations below the spectral width of the pulses is close to the temperature-defined energy spread in the ensemble, so the non-uniform character of the FC factors for continuum-bound transitions can in fact reveal itself. Nevertheless the SVCA provides a good estimate: the

Maxwell-Boltzmann statistical weight of the lowest energy states, which poses the highest challenge to the approximation, is small.

Within SVCA, $F_{corr}(\tau) = 2\pi\delta(\tau)$. This means that the size of the Frank-Condon window in phase space is small compared to the characteristic features of the continuum wavefunction. The population transferred by the field from the state $|2\rangle$ into continuum immediately leaves the FC window, and cannot be re-pumped back. Taking the integral involving F_{corr} in Eq.(8) (note that the integral is taken on the half, rather than whole, axis of time), yields the two coupled equations describing the dynamics of the bound states in the presence of the photoassociation pulses [3, 4]:

$$\dot{b}_1 = i \Omega_1^* b_2 e^{-i \Delta_1 t} \quad (11)$$

$$\dot{b}_2 = i \Omega_1 b_1 e^{i \Delta_1 t} - \Gamma b_2 + i \Omega_E F_0(t) \quad (12)$$

where $\Gamma \equiv \Gamma_f + \pi |\Omega_E|^2$.

Appearance of Equations (11,12), with the initial (continuum) state eliminated, is different from the one commonly used to describe bound-bound adiabatic transfer[1, 2]. Diagonalization of Eqs. (11,12), unlike that of the conventional equations for bound-bound passage, does not explicitly reveal the "dark" state connecting the initial and the target states of the system. Instead, the continuum acts as a source of population for the final state $|1\rangle$, with a very small transient population in the intermediate state $|2\rangle$ during the coherent "scooping" process. We choose this description versus the ones which replace the continuum by a single, decaying[2, 28] or non-decaying[5], level, since it allows to explicitly take into account the shape of the initial continuum wave packet. This approach is necessary when considering photoassociation with pulses, which coherently pumps up by the field at ω_2 a band of continuum levels of the width $\Delta E \sim \Delta\omega_2$, creating a "dark" wave packet on the background of the initial continuum state. Equations 6, 11 and 12 connect the shape of the wave packet scooped from the continuum with that of the laser pulses. For a given $F_0(t)$, representing the initial wave packet of continuum states, one can find, in principle, optimal pulses $\Omega_1(t)$ and $\Omega_E(t)$ that will photoassociate the entire population contained in it[29]. It has been demonstrated that a "counterintuitive" PAP sequence of Gaussian pulses, analogous to a bound-bound STIRAP sequence, can give rise to an almost complete population transfer in the $\text{Na}+\text{Na} \rightarrow \text{Na}_2$ photoassociation[3].

Figure 5 shows one simple example of photoassociation of a coherent Gaussian wave

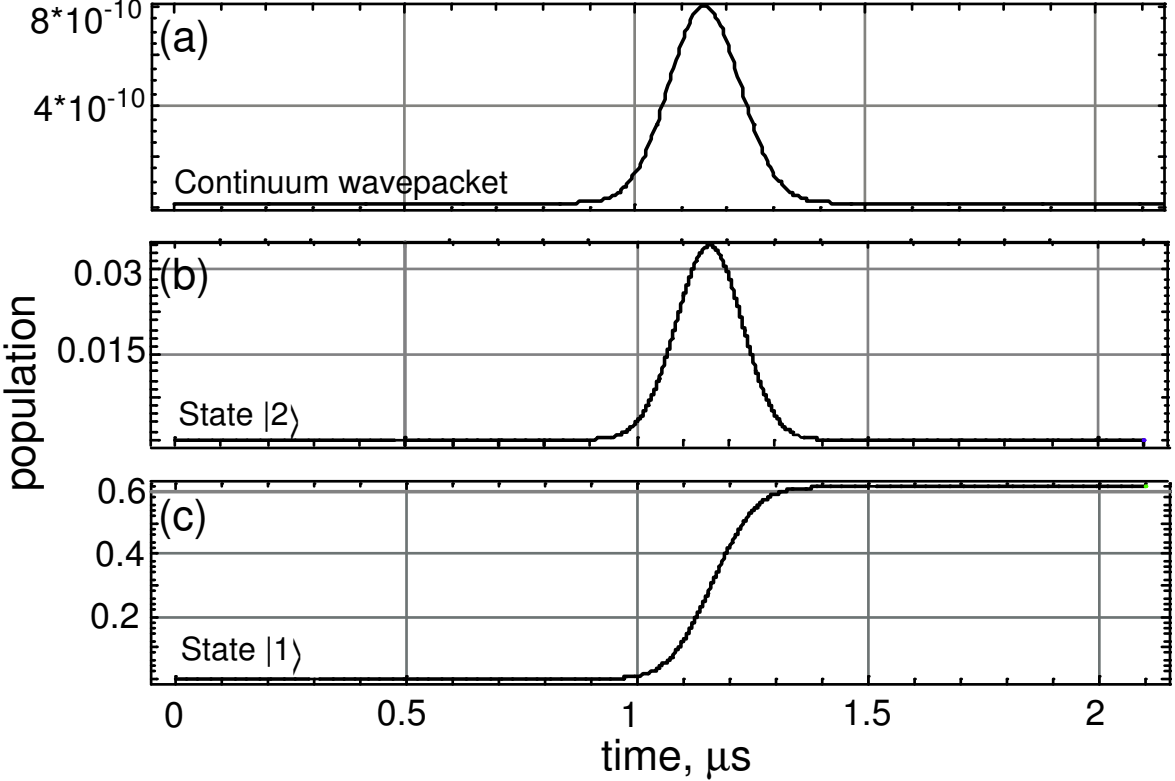


FIG. 5: Photoassociation of a coherent wave packet. (a) Initial continuum probability distribution $|F_0(t)|^2$, a.u.; (b) The population of the intermediate A/b state; (c) The population of the X($v = 4, J = 0$) target state.

packet in Rb, which is the shortest in time allowed by the temperature spread δE (transform limited wave packet). Intuitively this is the most classical scattering scenario allowed under the quantum law, where two atomic wave packets of minimal spread collide at time t_0 . The initial state is given by the superposition of the energy eigenstates

$$b_E(t = 0) = (\delta_E^2 \pi)^{-1/4} \exp [-(E - E_0)^2 / 2\delta_E^2 + i(E - E_0)t_0] \quad (13)$$

with $E_0 = 100 \mu K$, $\delta_E = 70 \mu K$, $t_0 = 1150$ ns. The pulse pair overlap time is chosen to match the coherence time of an atom-pair during collision at a given temperature and t_0 corresponds to the maximal overlap between the $\Omega_1(t)$ and $\Omega_E(t)$ pulses. The resulting continuum envelope $F_0(t)$ is shown in Fig. 5(a). In this calculation, the applied pair of laser pulses transfers the entire population of the continuum wave packet to the X($v = 4, J = 0$) state (of energy $E = -0.01823$ a.u.). The pair of pulses is composed of a σ^- polarized 733 nm Stokes pulse, whose intensity is 7×10^3 W/cm 2 , operating in resonance with $\omega_{2,1}$

transition frequency between the final $|1\rangle = \text{X}(v = 4, J = 0)$ state and the intermediate $|2\rangle = \text{A}/\text{b}(v = 133, J = 1)$ state. The second component is a σ^+ polarized pump pulse, operating in resonance with $\omega_{2,E}$ transition frequency between the intermediate $\text{A}/\text{b}(v = 133, J = 1)$ state. and the $\text{X}(E, J = 0)$ initial continuum state. The pump pulse, which is centered about 1063.4 nm, has intensity of 10^4 W/cm^2 . Both pulses are of 750 ns FWHM duration, with the pump delayed 600 ns relative to the Stokes pulse (the “counter-intuitive” order).

The pulse durations are chosen so that their spectral widths will roughly coincide with the initial continuum energy spread (which determines $F_0(t)$). As shown below, this fact ensures that the yield remains high even after thermal averaging at $T = 100 \mu\text{K}$ is performed.

Assuming a $\sin^2(\alpha t)$ - shaped pulses and setting $1/\Gamma_f = 30 \text{ ns}$, we numerically solve the Schrödinger equation from which the continuum has been adiabatically eliminated. As shown in Fig. 5, the final population of the $\text{X}(v = 4, J = 0)$ state is 0.6. When Γ_f is set to zero, $P(E)$, the transfer probability per collision may reach values as high as 0.9 for the same pulse configurations.

Once the $\text{X}(v = 4, J = 0)$ state is populated, it is easy to find an additional pair of pulses of variable intensities and center frequencies that can execute the transfer to the desired $\text{X}(v = 0, J = 0)$ state. An example of such a pair of pulses, applied right after the end of the first pair, is shown in Fig. 1(a). Both pulses are circularly polarized, 750 ns FWHM in duration, and have intensity of 10W/cm^2 . The transfer proceeds via an intermediate A/b vibrational state $|3\rangle$ of energy $E_1 = 0.03309 \text{ a.u.}$ The pump pulse of wavelength 888nm is followed after a delay of 600 ns by a Stokes pulse of wavelength 869.6nm. As we shall see, the population of the $\text{X}(v = 4, J = 0)$ state is completely transferred by this pair to the $\text{X}(v = 0, J = 0)$ state (state $|4\rangle$ in Fig. 6).

In order to estimate the fraction of atoms photoassociated per pulse-pair we need to multiply $P(E)$, the photoassociation probability per collision at energy E , by the number of collisions experienced by a given atom during the pulses (this is equivalent to averaging over all possible values of t_0). The number of collisions during the pulses is calculated as follows: At a given energy E , the velocity of a given atom is $v = (2E/m)^{\frac{1}{2}}$ and the distance traversed by it during a pulse of τ_{laser} duration is $v\tau_{laser}$. The cross-section for collision is πb^2 where b is the impact parameter, related to the J partial wave angular momentum as $b = (J + 1/2)/p = (J + 1/2)/(2mE)^{\frac{1}{2}}$. Hence, the number of collisions experienced by the

atom during the two pulses is $N = \rho\pi b^2 v\tau_{laser}$ where ρ is the density of atoms. Putting all this together we have for $J = 0$ that the fraction of atoms photoassociated per pulse-pair is

$$f(E) = \frac{P(E)\pi\rho(2E/m)^{\frac{1}{2}}\tau_{laser}}{8mE} = \frac{P(E)\pi\rho\tau_{laser}}{4m^{3/2}(2E)^{\frac{1}{2}}}. \quad (14)$$

When optimizing the photoassociation efficiency for an atomic ensemble, τ_{laser} is not a free parameter: bandwidth of the overlap of the pump and the Stokes pulses should match the energy spread in the ensemble kT . For $\tau_{laser} = 750$ ns, atomic density in an atomic trap of density $\rho = 10^{11} \text{ cm}^{-3}$, collision energy $E = 100 \mu\text{K}$, reduced atomic mass of $m = 1823 \times 85/2$ a.u., we have that $f \approx 4 \times 10^{-7}$ per pulse-pair.

As an alternative to the above estimate, one can repeat the calculations starting with an almost mono-energetic continuum wave packet that is spread over the average distance between two atoms experiencing an s-wave collision: $r_{st} = 1/(\pi\rho b^2)$. For a collision at $100 \mu\text{K}$ energy, and the atomic density in the trap equal to $\rho = 10^{11} \text{ cm}^{-3}$, we obtain $r_{st} = 4.21 \times 10^9$ a.u. From the uncertainty principle, one must set the energy spread of such wave packets to $\Delta E = \sqrt{E/2m r_{st}^2} = 1.07 \times 10^{-17}$ a.u. in Eq.(13). Then $F_0(t)^2 = 3.8 \times 10^{-17}$ a.u. at the time when the pulses are applied.

Since the wave packets are almost mono-energetic, it is now necessary to average the results of these calculations over the energy E of the Maxwell-Boltzmann thermal distribution:

$$P_{total} = \frac{2}{\sqrt{\pi}(kT)^{3/2}} \int_{E_{th}}^{\infty} dE P(E) \sqrt{E} \exp[-E/kT]. \quad (15)$$

For each energy the bound-continuum matrix element was obtained according to the data of Fig. 3, and the time dependent Shrödinger equation solved in the SVCA. The SVCA-based elimination of the continuum becomes less accurate as the collision energy tends to zero, but since the density of the continuum states vanishes at small energies, the contribution to the weighted signal from the low-energy collisions is small[30].

Fig 6 shows the ensemble-averaged populations of all the states involved in the scheme under the action of the two pulse pairs described earlier. The final population of the ground X state is equal to 2.13×10^{-7} . This number is lower than the one given by the simple estimate above, since in the realistic calculation the photoassociation takes place when the two pulses overlap, rather than during the full τ_{laser} . Thus one needs to repeat the pulse sequence about 5×10^6 times in order to photoassociate the entire ensemble, assuming that all the collisions take place on the $X^1\Sigma_g^+$ potential surface of the Rb_2 molecule. Approximately three

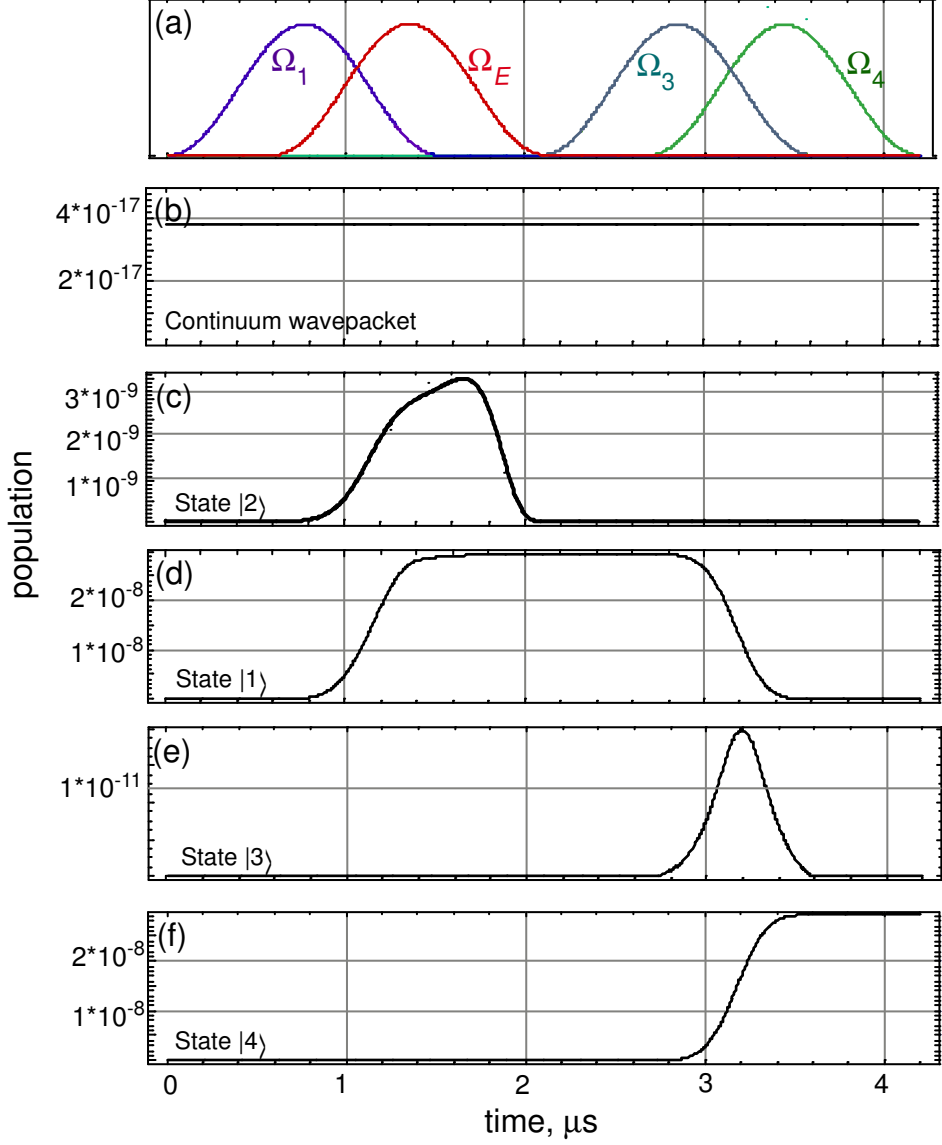


FIG. 6: (Color online). Photoassociation of the atomic ensemble in a trap. (a): Envelopes of the four laser pulses, unscaled. (b): Continuum population $F_0(t)^2$; (c)-(f): Bound state populations, weighted over the ensemble, for different bound states. (c): Intermediate state $|2\rangle \equiv A/b(v = 133, J = 1)$, $E = 0.042848$ a.u.; (d): State $|1\rangle \equiv X(v = 4, J = 0)$, $E = -0.01823$ a.u.; (e): Intermediate state $|3\rangle \equiv A/b(v = 35, J = 1)$, $E = 0.03309$ a.u.; (f): State $|4\rangle \equiv X(v = 0, J = 0)$, $E = -0.0193$ a.u.

quarters of the collisions occur on the $1^3\Sigma_u^+$ potential surface, and these are not affected in our arrangement due to the selection rules for transitions at the chosen frequencies. Accounting for the latter collisions, we multiply the above number by 4, and obtain that $\sim 2 \times 10^7$ pulses

are required for complete photoassociation.

When we come to estimate the maximal rate at which the photoassociation pulse sets can be sent into the cold atomic cloud, it is necessary to appreciate the need to avoid excitation and heating by subsequent pulse sets of the molecules already created. In order to accumulate a large number of cold molecules, the molecules must be removed from the beam path of the light after every set of pulses before the next set of pulses can be sent in. This requirement poses an inherent limit on the actual repetition rate of a possible experiment, which depends on the mechanism used to remove the molecules. The simplest possibilities of thermal diffusion / gravitational fall are slow processes, and would limit the repetition time to 1-10ms. Faster mechanisms may require application of mechanical forces on the molecules (but not the atoms) to push them out of the beam. An example for a pushing mechanism can be a fast moving optical lattice, made up of two counter propagating waves of slightly different frequencies. Suppose that we deal with an elongated trap, $\sim 20\mu\text{m}$ in diameter, and $\sim 200\mu\text{m}$ long. Let us send in a slowly moving optical lattice, oriented parallel to the long dimension of the trap, moving with the speed of 20 cm/s (thermal velocity at the $100\mu\text{K}$ temperature). The lattice with the period of $1\mu\text{m}$ is designed to hold only molecules (without heating) but not atoms. A single pulse sequence will place about 20 molecules into every $1 \times 1 \times 200 \mu\text{m}$ slot of the lattice overlapping with the trap. The next similar pulse sequence can be applied 100 μs later, when the molecule-loaded lattice slots leave the trap.

The inherent inefficiency of the photoassociation process in the pulsed regime is due to the fact that one has to operate within the coherence time of the ensemble, hiding the created molecules away before the next pulse sequence arrives. Our results are to be compared with those for creation of ground state molecules with CW lasers. In the seminal experiment [31], the ground state molecules were created with the estimated rate of about 500 molecules per second (since the molecules were not trapped, the actual detection rate was lower). This value can be, in principle, increased; there is a constraint on the effectiveness of the CW photoassociation lying in the fact that it incoherently populates many highly excited vibrational states, as well as molecular continuum.

The estimate (14) trivially scales with the temperature and the density of the atomic sample. In the case of photoassociation at either BEC [7] or Mott insulator [32] conditions one can hope to photo-associate the whole sample with a single sequence of pulses.

Unlike bound-bound STIRAP, the continuum-bound REAR process continues to work

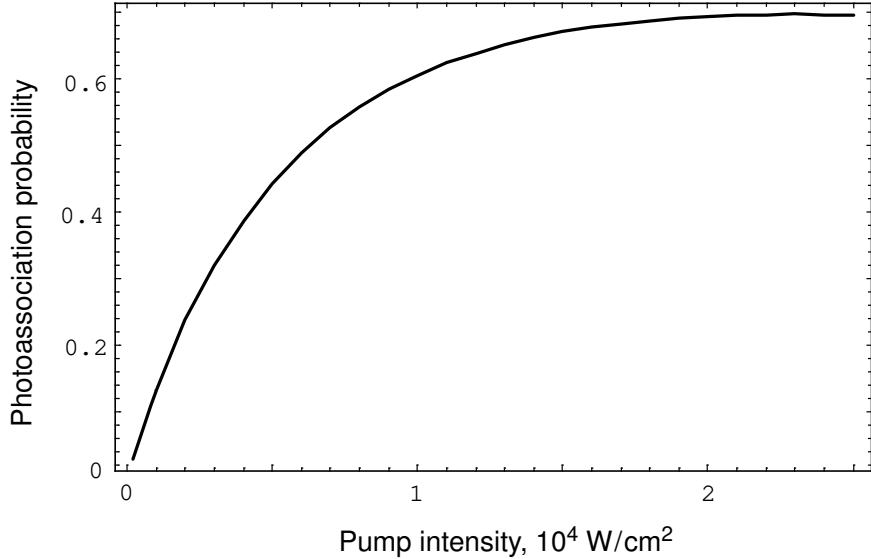


FIG. 7: Final population of the state $X(v = 4, J = 0)$ in photoassociation of a coherent wave packet in dependence on the pump pulse intensity.

even if the laser intensity is not sufficient for the complete population transfer. This can be seen from Eq. (12). Apart from modifying the rate of decay of the intermediate level, the pump Rabi frequency Ω_E enters the Schroedinger equation only in combination with the initial continuum envelope F_0 . Reducing the pump Rabi frequency is roughly equivalent to reducing the amplitude of the initial scattering state, and does not influence the passage itself.

We repeated the calculation presented in Fig. 5 for a set of the pump intensities below and above 10^4 W/cm^2 . The results are shown in Fig. 7. As expected, the photoassociation probability at low intensities roughly scales as square root of the intensity. In each simulation the probability of populating the intermediate $A/b(v = 133, J = 1)$ state was much lower than the final photoassociation probability, and the general time dependance of the bound state populations was similar to that shown in Fig. 5.

Thus even in situations when the FC factors are too low for the complete population transfer, a REAR photoassociating pulse pair allows to scoop from the continuum a part of its population, and to transfer it, almost without losses, onto the bound molecular state.

IV. CONCLUSIONS.

We have demonstrated that one can implement AP in photoassociation in a thermal ensemble of cold atoms. AP is best implemented when the bandwidths of the laser pulses involved are slightly narrower than the energy spread of the ensemble. In this way, the REAR process works for any initial continuum energy.

The number of pulses needed to complete the photoassociation depends only on the ratio between the coherence time and the average time between s-wave collisions. Our estimate for the number of pulses needed to photoassociate an entire ensemble of $100 \mu\text{K}$ Rb atoms at density of 10^{11} cm^{-3} is 2×10^7 . The exact number can vary depending on whether one photoassociates atoms colliding on the singlet (as we have done) or the triplet potential surfaces.

The requirement that the photoassociating pulse sequence works the same way for all the initial energies in the ensemble is generic for any coherent photoassociation scheme. If simple laser pulses are used, this means that the pulse durations must not exceed the coherence time in the ensemble by much. The AP sequence considered in this paper photoassociates almost all the continuum population that passes through the FC region during the coherence time window. Thus, for simple-structured pulses, the AP sequence places the upper boundary on what is possible to achieve. Use of more complex pulse shapes, such as the numerically optimized shapes in Ref. [21], is limited in our scheme by the requirement that the laser spectrum be smooth on the scale of the ensemble thermal energy spread.

We conducted our simulations for singlet collisions of Rb⁽⁸⁵⁾ atoms. Due to the pole in the scattering length, the FC factors are strongly enhanced, and the required intensities are quite low. The scheme needs 10^4 W/cm^2 intensity for the continuum-bound 1063.4 nm pump pulse; all the other intensities are adjustable, and are below this number.

Once the continuum state is transferred onto a vibrationally excited bound state of the ground electronic surface, it is relatively easy to employ another AP pulse pair transferring the population to the ground ro-vibrational state.

In an analogy with weak-field coherent control (CC)[4], interference of quantum pathways for the system following several dark states can either enhance or suppress the probability of photoassociation. Combining the vast possibilities of coherent control with the ability to adiabatically transfer 100% of quantum population into the desired state [2] would give a

powerful tool for quantum engineering. Progress in this direction has been made in controlling bound-bound population transfer [10].

We have numerically investigated the dark state interference for free-bound transitions, for two basic configurations involving an initial continuum – the “double- Λ ” (PAP via two different intermediate states) and the “tripod” (PAP into a superposition of two final states) linkages. In both cases the branching ratios and the effectiveness of the population transfer for the continuum-bound processes coincided with those expected from the bound-bound multi-pathway STIRAP [2, 10]. Coherently Controlled Adiabatic Passage, if implemented in photoassociation, can provide the means to implement a number of exciting schemes based on the continuum-bound pathway interference. As an example, it is possible to measure the multi-channel continuum state in the trap by photoassociating a desired multi-channel wave packet (such as either even or odd superposition of single-channel components, either even or odd temporal structure, etc.) at a given moment and leaving aside all orthogonal waveforms [29]. Some work in this direction will be presented elsewhere.

V. ACKNOWLEDGMENTS.

The authors thank S. Lunell and D. Edvardsson for sharing the output data of their calculation [12]. We acknowledge fruitful discussions with M. Stowe, T. Zelevinsky, K. Madison, and D. Jones. E. Shapiro is pleased to thank I. Thanopulos for discussions and numerical advice. The work at JILA is funded by NSF and NIST. A. Pe'er thanks the Fulbright foundation for financial support.

- [1] J. Oreg, F.T. Hioe, J.H. Eberly, Phys. rev. A **29**, 690 (1984); U. Gaubatz *et. al.*, J. Chem. Phys. **92**, 5363 (1990);
- [2] N.V. Vitanov *et. al.*, Adv. At. Mol. Opt. Phys. **46**, 55 (2001), and references therein.
- [3] A. Vardi *et. al.*, J. Chem Phys. **107**(16) 6166 (1997)
- [4] M. Shapiro and P. Brumer, ”Principles of the Quantum Control of Molecular Processes” John Wiley & Sons, New Jersey, 2003.
- [5] M. Mackie, J. Javanainen, Phys. Rev. A **60**, 3174 (1999).

[6] A. Vardi, M. Shapiro, J.R. Anglin, Phys. Rev. A **65**, 027401 (2002); J. Javanainen and M. Mackie, *ibid.* **65**, 027402 (2002).

[7] M. Mackie, R. Kowalski, J. Javanainen, Phys. Rev. Lett. **84** 3803 (2000); P.D. Drummond *et. al.*, Phys. Rev. A **65** 063619 (2002); H.Y. Ling, H. Pu, B. Seaman, Phys. Rev. Lett. **93** 250403 (2004).

[8] R. Dumke *et. al.*, Phys. Rev. A **72**, 041801(R) (2005).

[9] K. Winkler *et. al.*, Phys. Rev. Lett. **95**, 063202 (2005).

[10] P. Kral, I. Thannopulos, M. Shapiro, "Coherently controlled adiabatic passage", Rev. Mod. Phys., in press, and references therein.

[11] I. Thannopulos, M. Shapiro, in preparation

[12] D. Edvardsson, S. Lunell, and C.M. Marian, Molecular Physics

[13] M. Marinescu, H.R. Sadeghpour, A. Dalgarno, Phys. Rev. A **49**, 982 (1994).

[14] J.L. Roberts *et. al.*, Phys. Rev. Lett. **81**, 5109 (1998); J.M. Vogels *et.al.*, Phys. Rev. A **56** R1067 (1997).

[15] L.D. Landau, E.M. Lifshitz, "Quantum mechanics: Non-relativistic theory", Butterworth-Heinemann, Oxford (1981).

[16] J. Weiner *et. al.*, Rev. Mod. Phys. **71** 1 (1999).

[17] F. Spiegelmann, D. Pavolini, J.-P. Daudey, J. Phys. B: At. Mol. Opt. Phys. **22**, 2465 (1989).

[18] M. Shapiro, J. Chem. Phys. **56** 2582 (1972).

[19] C. Gabbanini *et. al.*, Phys. Rev. Lett. **84** 2814 (2000); M. Kemmann *et. al.*, Phys. Rev. A **69** 022715 (2004).

[20] E. Luc-Koenig, M. Vatasescu, F. Masnou-Seeuws, Eur. Phys. J. D **31** 239 (2004).

[21] C.P. Koch *et al.*, Phys. Rev. A **70**, 013402 (2004).

[22] W. Salzmann *et. al.*, Phys. Rev. A **73** 023414 (2001).

[23] B.L. Brown, A.J. Dicks, I.A. Walmsley, physics/0509109 (2006).

[24] A.G. Abraskevich, D.G. Abraskevich, Computer Physics Communications **82**, 193 (1994); *ibid.*, **82**, 209 (1994).

[25] M.S. Safronova, W.R. Johnson, A. Derevianko, Phys. Rev. A **60**, 4476 (1999).

[26] M. Shapiro, J. Chem. Phys. **101**, 3844 (1994).

[27] E.A. Shapiro, Sov. Phys. JETP **118**, 516 (2000); Laser Physics **12** 1448 (2002).

[28] M.N. Kobrak, S.A. Rice, J. Chem. Phys. **109**, 1 (1998).

- [29] E.A. Shapiro and Moshe Shapiro, in preparation.
- [30] It turns out that adjusting the matrix elements according to the Wigner $E^{1/4}$ law rather than the resonance law would only insignificantly decrease the final temperature-weighted population of the ground state.
- [31] J.M. Sage *et.al.*, Phys. Rev. Lett. **94** 203001 (2005).
- [32] M. Gelner *et. al.*, Nature **415** 39 (2002); D. Jaksch *et. al.*, Phys. Rev. Lett. **89** 040402 (2002).
- [33] D. Jaksch *et. al.*, Phys. Rev. Lett. **85** 2208 (2000); I.R. Sola, V.S. Malinovsky, J. Santamaria, J. Chem. Phys. **120** 10955 (2004).